

UNIVERSIDADE DE SANTIAGO DE COMPOSTELA



FACULTAD DE FÍSICA  
Departamento de Física de Partículas

**Simulation of the light detection for the  
optimization of CALIFA crystals**

Memoria presentada por:  
**Paloma Díaz Fernández**  
como disertación para optar al  
**Diploma de Estudios Avanzados**  
Junio 2010



# UNIVERSIDADE DE SANTIAGO DE COMPOSTELA

El Doctor Héctor Álvarez Pol, Profesor Titular del Departamento de Física de Partículas de la Universidad de Santiago de Compostela,

## INFORMA:

que la memoria titulada **Simulation of the light detection for the optimization of CALIFA crystals** ha sido realizada bajo su dirección por **Paloma Díaz Fernández** en el **Departamento de Física de Partículas** de esta **Universidad**, y constituye el **Trabajo de Investigación Tutelado** que presenta para optar al **Diploma de Estudios Avanzados**.

Santiago de Compostela, a 18 de Mayo de 2010.

Fdo. Héctor Álvarez Pol

Fdo. Paloma Díaz Fernández



# Contents

<b>1</b>	<b>Introduction</b>	<b>1</b>
1.1	Motivation . . . . .	1
1.1.1	Present work . . . . .	2
<b>2</b>	<b>The propagation of light</b>	<b>3</b>
2.1	Basic optical concepts. . . . .	3
2.2	Optics in Geant4 . . . . .	5
2.2.1	Geant4 models . . . . .	5
2.2.2	Possible processes . . . . .	7
<b>3</b>	<b>Simulation</b>	<b>9</b>
3.1	R3BSim. . . . .	9
3.2	Crystal geometries used in the simulation. . . . .	10
3.3	Main features of the simulations performed. . . . .	12
<b>4</b>	<b>Results of the simulation</b>	<b>13</b>
4.1	Study of the light propagation in the crystal with Geant4. . . . .	13
4.2	Simulation of the crystal prototypes. . . . .	25
4.2.1	Dependences with the light guide angle for a source of gammas. . . . .	27
4.2.2	Dependences with the light guide angle for a source of photons. . . . .	32
<b>5</b>	<b>Conclusions</b>	<b>43</b>



# Chapter 1

## Introduction

### 1.1 Motivation

Light behaviour and its propagation in scintillators are, among other parameters, relevant for the optimization of crystals design; in particular a better energy resolution could be achieved when the light collection is improved. The goal of this work is to study the geometry of the light guides to optimize the number of detected photons, which improves the light collection in the prototype crystals of the calorimeter CALIFA (CALorimeter for In-Flight emitted gAmmas) designed by the GENP<sup>1</sup>. This calorimeter will be installed in the new facility FAIR<sup>2</sup>[2] in the R<sup>3</sup>B setup (see figure 1.1).

The aim of the R<sup>3</sup>B international collaboration is to develop and construct a versatile reaction setup with high efficiency, acceptance, and resolution for kinematically complete measurements of reactions with high-energy radioactive beams. The setup will be located at the focal plane of the high-energy branch of the Super-FRS<sup>3</sup>.

The CALIFA calorimeter is a detector formed by crystals of CsI (Tl). The scintillation material and the readout device are ingredients that would determine the energy resolution of the detector. Simulations are essential to define the crystal's geometry. Light collection is affected by changes in the wrapping and the crystal's surface finish. The study of the light propagation inside the crystals makes possible to improve the crystal's design. Check the effect of the light guide geometry in the most typical scenarios is a useful

---

<sup>1</sup>Grupo experimental de núcleos y partículas of the Universidade de Santiago de Compostela (<http://www.usc.es/genp/>).

<sup>2</sup>Facility for Antiproton and Ion Research.

<sup>3</sup>The Super-FRS is a large-acceptance superconducting fragment separator followed by different experimental branches including a combination with a new storage-cooler ring system.

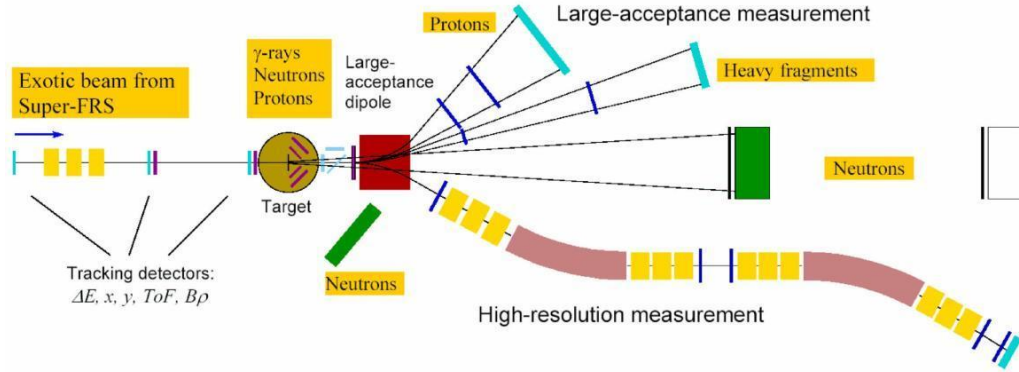


Figure 1.1: Schematic experimental R3B experiment at FAIR setup.

tool to improve the light collection.

### 1.1.1 Present work

After this brief introduction we will describe in the second chapter some optical definitions necessary to understand this work. First, we introduce some generic optical characteristics and then its application in the Geant4 code. In the third chapter we will describe the simulation package R3BSim and its application in this work. The geometries used in this work and their main features will be described too. In the fourth chapter the simulation results will be presented. In first place we will talk about some simulations performed with a simply geometry to check the Geant4 optical model. In secondly we will describe the results obtained in order to fix some parameters of the model and in the last part we will show the results obtained using the prototype designed by the GENP and a study of how some changes in the geometry influence the light collection. Conclusions will be briefly outlined in the last chapter.

# Chapter 2

## The propagation of light

In this chapter some optical concepts are presented. First we present these concepts from the point of view of the optical theory and in second place we show the Geant4 treatment.

### 2.1 Basic optical concepts.

The light can suffer in matter different phenomena. When the light finds two mediums with different optical properties some processes could take place. We are going to study here the most important: transmission, reflection and refraction. So, in this section some basics concepts are going to be described.

When a beam of light strikes such an interface<sup>1</sup>, a part of the light is always scattered back, this phenomenon is called **reflection** [1]. The first part of the Fresnel law of reflection says: “The angle of incidence is equal to the angle of reflection”. If the reflecting surface is very smooth, the reflection of light that occurs is called *specular or regular reflection*. When light strikes a rough or granular surface, it bounces off in all directions due to the microscopic irregularities of the interface. This is called *diffuse reflection* (see figure 2.1).

**Refraction** is the change in direction of a wave due to a change in its speed. Refraction is described by Snell’s law, which states that the angle of

---

<sup>1</sup>An optical interface is a thin layer or boundary between two different substances or two phases of a single substance. For example, if water and oil are mixed together, they tend to separate, and at equilibrium they are in two different strata with an oil-water interface in between. The surface of a lake is a water-air interface.

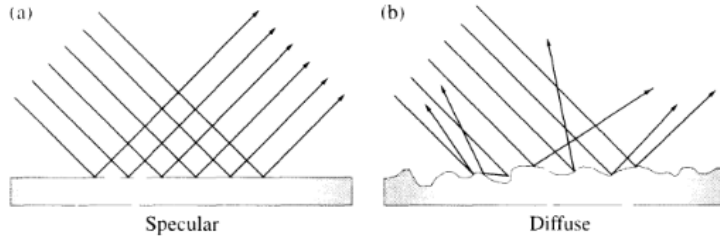


Figure 2.1: (a)Specular reflection. (b)Diffuse reflection.

incidence  $\theta_i$  is related to the angle of refraction  $\theta_r$  by

$$\frac{\sin \theta_i}{\sin \theta_r} = \frac{v_i}{v_r} = \frac{n_r}{n_i} \quad (2.1)$$

Two important facts are the following: the ray that enters in a medium with higher index bends towards the normal while when this ray enters a medium with lower index, it bends away from the normal (see figure 2.2).

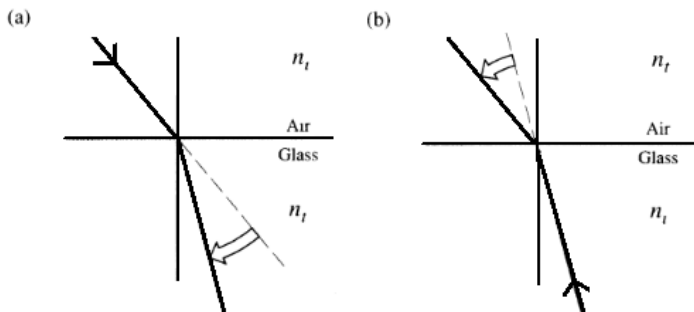


Figure 2.2: The bending of rays at an interface. (a)When a beam of light enters a more optically dense medium it bends towards the perpendicular. (b)When a beam goes from a more dense to a less dense medium, it bends away from the perpendicular.

**Total internal reflection** is an optical phenomenon that occurs when a ray of light strikes a medium boundary at an angle larger than a particular critical angle with respect to the normal to the surface. If the refractive index is lower on the other side of the boundary, no light can pass through and all of the light is reflected. The critical angle (see equation 2.2) is the angle of incidence above which the total internal reflection occurs (see figure 2.3).

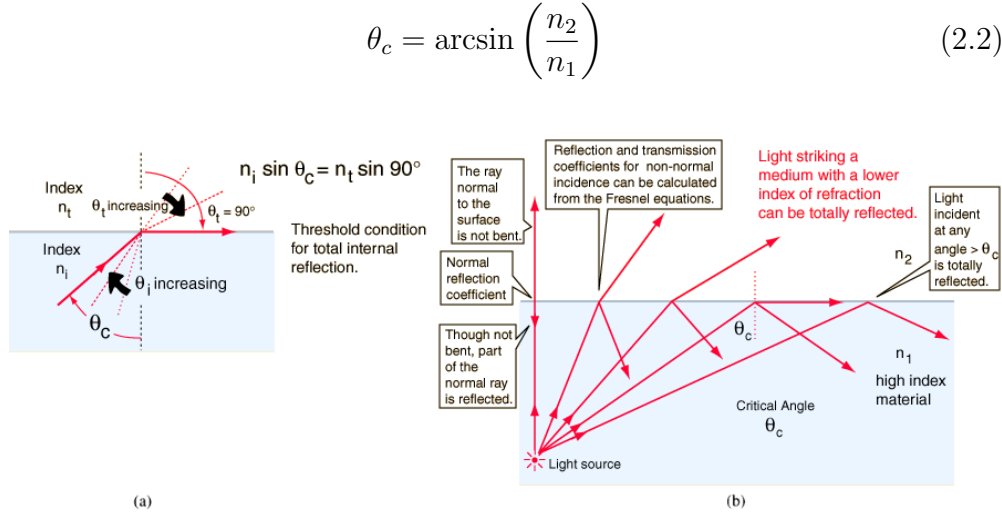


Figure 2.3: Total internal reflection and critical angle. (a) Threshold condition of total internal reflection. (b) Different reflection types for different incident angles. Figure taken from [7].

## 2.2 Optics in Geant4

In this section we focus in the Geant4 description of the optical processes. Fully information can be read in the bibliography given along the text.

### 2.2.1 Geant4 models

Geant4 can realistically model the optics of scintillation. The Geant4 code allows the user to select between two optical reflections models, the *GLISUR model*<sup>2</sup> and the *UNIFIED model*<sup>3</sup> [6]. We are going to select the unified model, because the glisur model is more limited in the treatment of the surface wrappings. The glisur model assumes that the surface is made of micro-facets, where a micro-facet is randomly selected from a distribution each time a reflection occurs. The micro-facet normal is calculated as the

<sup>2</sup>The original GEANT3.21 implementation of this process is also available via the GLISUR methods flag.

<sup>3</sup>[A. Levin and C. Moisan, A More Physical Approach to Model the Surface Treatment of Scintillation Counters and its Implementation into DETECT, TRIUMF Preprint TRI-PP-96-64, Oct. 1996] of the DETECT program [G.F. Knoll, T.F. Knoll and T.M. Henderson, Light Collection Scintillation Detector Composites for Neutron Detection, IEEE Trans. Nucl. Sci., 35 (1988) 872.].

sum of two vectors; the average surface nominal normal, and a second vector, which is defined by a random point on a sphere of radius  $(1 - \textit{polish})$ , with  $\textit{polish} \leq 1$ , and added to the tip of the first vector. A specular reflection is thereafter calculated based on the micro-facet orientation. In all the tests we choose the unified model, this one has more possibilities in the finish options, for example. Next, we are going to describe the main features of the unified model. More information can be obtained in [4], [5] and in [6].

In the *unified model* four kinds of surface reflection are possible: specular spike, specular lobe, backscatter and lambertian. In the **specular spike reflection** the photon is reflected around the average surface normal. For a **specular lobe reflection**, the surface is assumed to be made of micro-facets which are oriented around the average surface with a gaussian distribution. The standard deviation of the distribution of the micro-facets orientation is defined by a parameter called **sigmaalpha**. Each time a specular lobe reflection happens, a micro-facet is randomly selected and a specular reflection is calculated based on the micro-facet orientation. In case of **backscatter reflection**, the photon is reflected back into the direction the photon came from. For **lambertian reflection** the photon is reflected with a lambertian distribution (into a cosine distribution around the average normal). If a surface exhibits Lambertian reflectance, light falling on it is scattered such that the apparent brightness of the surface to an observer is the same regardless of the observer's angle of view. Lambertian reflection is often used as a model for diffuse reflection. In the figure 2.4 we have the four kinds of reflection schematically represented.

When a photon arrives at a medium boundary its behavior depends on the nature of the two materials that conform it. Medium boundaries may be formed between two dielectric materials or a dielectric and a metal. We need to set the surface type and the possibilities are: dielectric-dielectric (choice for the crystal) and dielectric-metal (typical choice for the detector). The main difference between a dielectric-dielectric and a dielectric-metal is that in the second one, photons are not expected to propagate inside due to the lack of index of refraction. Another parameter is the surface finish, that is the allowed deviation from a perfectly flat surface that is made by some manufacturing process. Combinations of surface finish properties, such as polished or ground and front painted or back painted, enumerate the different situations which can be simulated. Depending on the selected surface type we have different possibilities of the finish. Next we enumerate the different finish for each surface type:

- dielectric-dielectric: polished, polishedbackpainted, polishedfrontpainted, ground, groundbackpainted and groundfrontpainted.

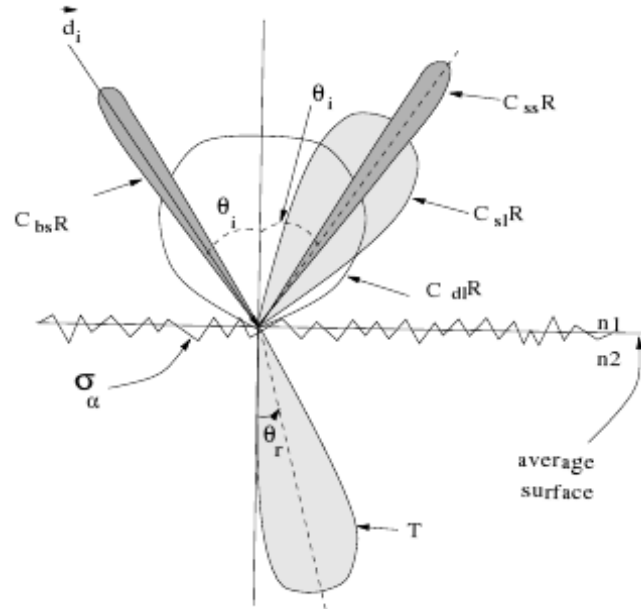


Figure 2.4: Polar plot of the radiant intensity in the *unified model*. This figure was extracted from the article [4], where a complete reference of the notation of the unified model is presented.

- dielectric-metal: polished and ground.

One needs to specify too the refractive index of the two materials, the reflectivity of the reflector attached to the surface, the probabilities of the four kinds of reflections and, in case it is used, the sigmaalpha constant.

## 2.2.2 Possible processes

The possible processes in the surface depends of the finish, because each type represents a real case. For a polished surface, photons can undergo fresnel reflection, total internal reflection and refraction. In case that you have a polishedbackpainted surface, polished back paint/foil, the possibilities are lobe reflection, spike reflection, backscatter reflection, lambertian reflection, refraction and absorption. If you set poshishedfrontpainted, polished top-layer paint, photons can undergo lobe reflection, spike reflection, backscatter and lambertian and absorption. For a ground surface, i.e. a rough surface, the possible processes are lobe, spike, backscatter, lambertian reflections, and it refraction is possible too. Setting a groundbackpainted surface, a rough back paint/foil, the processes are lobe, spike, backscatter

and lambertian reflections, refraction and absorption. In case that you have a groundfrontpainted, rough top-layer paint, the possibilities are lambertian reflection and absorption.

# Chapter 3

## Simulation

The aim of this chapter is to describe how the simulation of the light propagation on a prototype crystal of the calorimeter CALIFA (CALorimeter for In-Flight emitted gAmmas) has been performed. This chapter contains three sections. In the first one, we introduce the simulation code that has been used. In the second we explain the geometry of the crystals and in the last one we will see the particular features of our simulations.

### 3.1 R3BSim.

R3BSim is a simulation code particularly developed for the future R3B setup at FAIR[2]. R3BSim is a pure GEANT4<sup>1</sup> (G4)-ROOT<sup>2</sup> program that features a multihit data structure ready for event analysis and a modular geometry description that allows the integration of new detectors.

The program is written in C++; ROOT libraries are included allowing a fully integrated analysis interface: all the detectors are in a single TTree with individual branches for every detector, each one made of collections of detector hits (TClonesArray).

The simulation includes a large set of materials for the detectors and the passive elements that can be easily exchanged when needed. It has a

---

<sup>1</sup>Geant4 (for GEometry ANd Tracking) is a platform for “the simulation of the passage of particles through matter”, using Monte Carlo methods. It is the successor of the GEANT series of software toolkits developed by CERN, and the first to use Object oriented programming (in C++). Its development, maintenance and user support are taken care by the international Geant4 Collaboration. Application areas include high energy physics and nuclear experiments, medical, accelerator and space physics studies. The software is used by a number of research projects around the world (<http://geant4.web.cern.ch/geant4/>).

<sup>2</sup>ROOT is an object-oriented framework aimed at solving the data analysis challenges of high-energy physics (<http://root.cern.ch>).

messenger, for users that allow to do important changes in the configuration during the execution of the program (no need to recompile).

Regarding the physical processes, G4 allows and enforces a full customization of the physics description, providing different physics lists that can be chosen by the user, for electromagnetic processes, hadronic, ect.

Once we have a realistic description of the experimental setup and the physics, we need to simulate the incoming particles or beam. For that purpose, different event generators are available, like for instance single particles (protons, neutrons, gammas, ...) at different conditions (initial point, direction, energy, ...). Other more complicated generators could be developed; in particular in this work we have designed some generators that are going to be detailed in the next sections.

## 3.2 Crystal geometries used in the simulation.

Two different geometries have been used in order to perform the simulations. The first one was a simple box of variable dimensions, as we see in figure 3.1. We used this geometry to test the surface finish and to understand the behaviour of the Geant4 optical model.

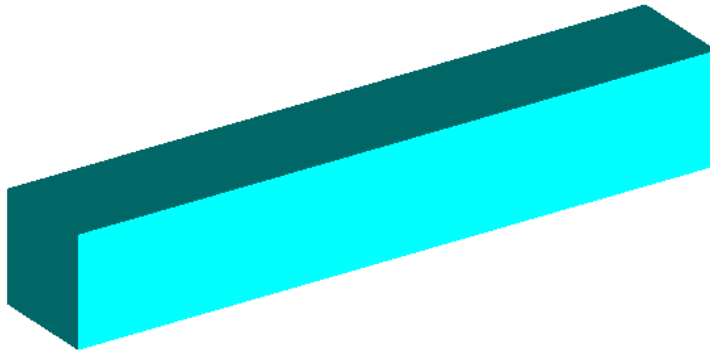


*Figure 3.1:* Figure of one of the different boxes used.

The second shape corresponds to the prototype crystals for the CALIFA calorimeter, designed by the GENP<sup>3</sup>. We used this geometry to study how the light guide angle affects to the light collection (see figure 3.2). These crystals are formed by two pyramidal truncated structures with rectangular

---

<sup>3</sup>Grupo experimental de núcleos y partículas of the Universidade de Santiago de Compostela (<http://www.usc.es/genp/>).

bases (see figure 3.3). The length of these crystals is 130 mm. The area of the entrance face is  $29 \times 10.4 \text{ mm}^2$ . The area where the APD is placed is  $19.8 \times 9.8 \text{ mm}^2$ .

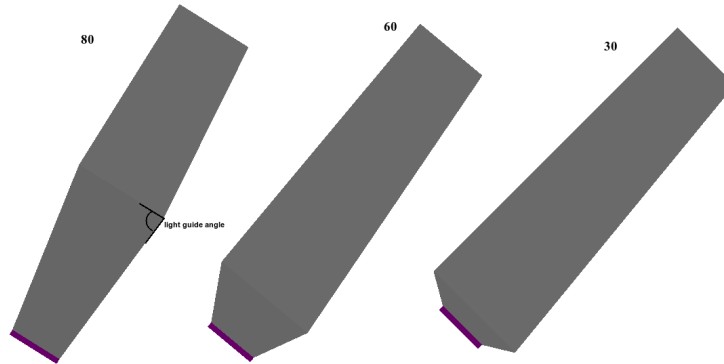


*Figure 3.2:* View of the prototype with different angles for the light guide.

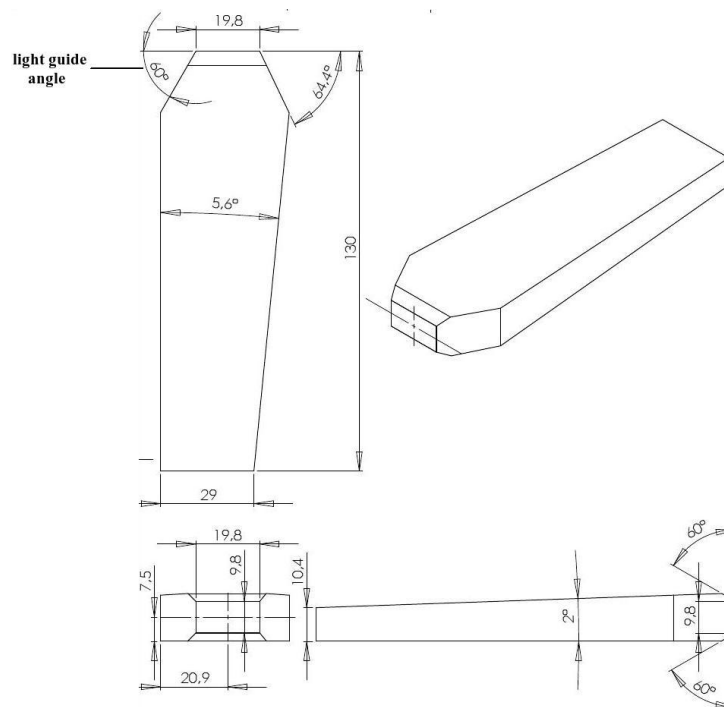


*Figure 3.3:* View of the prototype crystal for the calorimeter CALIFA.

### 3.3 Main features of the simulations performed.

In the preparation of an experiment the use of adequate simulation tools is a key issue to check some features of the experiment. We are going to divide this section in two parts. In the first one, we are going to study the unified model in Geant4, and in the second, the shape of the crystals in order to obtain a better light collection.

In the first case, to study the Geant4 optical treatment we used a parallelepiped crystal (see figure 3.1). The simulated optical photons source was a  $4\pi$  emission cube of  $1mm^3$  in the center of the crystal. The number of photons was  $10^4$  with an energy of 3 eV. These tests have been performed using different surface finish. To check the results under different wrapping and lapping characteristics, we used polished, polishedbackpainted, polished-frontpainted, ground, groundbackpainted and groundfrontpainted.

In the second case we study how the light guide angle affect the light collection. The simulated gamma source was placed at  $30mm$  from the entrance face. The source dimensions are chosen to be the same as the entrance face ones and the gammas are emitted along the longitudinal crystal axis. These gammas arrive to the crystal and produce optical photons by scintillation. The number of photons generates, depends on the value of one parameter called *scintillation yield*. In our case the value was  $54000/MeV$  (extracted from the data-sheet of Saint Gobain CsI crystals[13]). The *resolution scale* is a Geant4 parameter which broadens the statistical distribution of generated photons. Another parameters associated to the CsI material are: the *refraction index* of the CsI (1.79 for all the energy range) (taken from Saint Gobain data-sheet), the *absorption length* (taken from Litrani code). A scintillator is also characterized by its photon emission spectrum and by the exponential decay of its time spectrum. In Geant4 the scintillator can have a fast and a slow component. The relative strength of the fast component as a fraction of total scintillation yield is given by the *yield ratio*. One can specify too the *fast* and the *slow* time constants (all these taken from Saint Gobain data-sheet[13]). To check the results under different wrapping and lapping characteristics, we used for the surface between the crystal and the air the polishedbackpainted and groundfrontpainted finishes, for being these types very different. One is a specular reflector and the other is a diffuse reflector. We tried to use extremal cases to verify the behaviour of the light collection changing the light guide angle. For the interface between the crystal and the detector we used as surface type dielectric-metal and for the finish ground.

In the next chapter we will focus in the details.

# Chapter 4

## Results of the simulation

In this chapter some results obtained are presented. The first results were obtained with simulations performed with a parallelepiped of dimensions  $20 \times 20 \times 120 \text{ mm}^3$ , we use this geometry to study the light propagation in crystals with different finish. The second results shown were obtained from simulations performed with a crystal prototype of the CALIFA and the aim was study the influence of the light guide angle in the number of detections using different simulated sources.

### 4.1 Study of the light propagation in the crystal with Geant4.

To use the simulation as a tool for the optimization and prediction of the crystals behaviour, we need to understand the optical part of the Geant4 code. With this aim we are going to study individually each surface finish. As we have seen in the previous chapters once you choose a surface type some concrete finishes are associated to this one, and for each one, some processes can take place. Each finish tries to represent a real case of scintillator with or without wrapping. Two are the main options: a polished finish that tries to represent a scintillator with a polished surface and a ground finish which tries to represent the scintillator with an unpolished surface, both without any wrapping. These two main options can be combined with different wrapping configurations: a) using a diffuse reflector, like mylar aluminized (polished-front-painted and the ground-front-painted finishes); b) using a specular reflector, like teflon (polished-back-painted and ground-back-painted).

To study the propagation of the light, we perform a few simulations. The scintillator material is defined in the simulation using a box-like volume

with dimensions  $20 \times 20 \times 120 \text{ mm}^3$ . The simulated source emit  $10^4$  optical photons in all directions, from a volume of  $1 \times 1 \times 1 \text{ mm}^3$  placed inside the crystal and centered. The emitting point varies as well randomly inside the  $1 \times 1 \times 1 \text{ mm}^3$  cube. As a result of this simulation, we study a few observables: process type, incident and outgoing angles when a photon hits a surface and the difference between these angles. The variable process type have the information about how many times a process happens. The incident angle of a photon in an interface is the angle of the incoming direction respect to the surface normal. The outgoing angle of a photon in an interface is the angle of the photon after being refracted or reflected respect to the surface normal. The difference between these angles is just the subtraction between the outgoing and incoming angles.

### Study of the different surface finish.

The surface finishes availables in the unified model are categorized in two groups: polished and unpolished. These two main options can be combined or not with different wrapping configurations given the six possibilities for the finishes. We have three cases of polished surfaces and three cases for the ground surfaces, as we have seen in the introduction of this section. The difference between the “backpainted” and “frontpainted” options is that in the first one there is a gap between the crystal and the paint.

#### Polished:

##### POLISHED

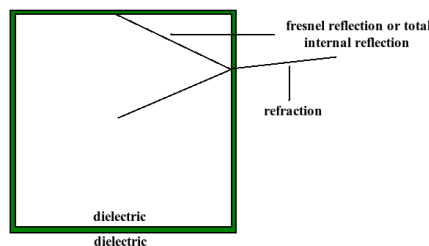


Figure 4.1: Schematic paint of a polished surface.

The polished finish tries to represent a real case of scintillator with a polished surface and without wrapping, is a naked crystal. In a smooth perfectly polished surface (between two dielectric media) three processes are

#### 4.1 Study of the light propagation in the crystal with Geant4. 15

possible: reflection, total internal reflection and refraction. The designation for the finish “polished” trumps any specification related to finish “ground” (e.g. the probabilities of the various UNIFIED model reflections, for example specular lobe, and hence also the specification of sigmaalpha to sample the facet normal). Thus, so long as you specify “polished”, some variables are not used by the code. For example no matter any sigmaalpha that you specify because the program is going to ignore.

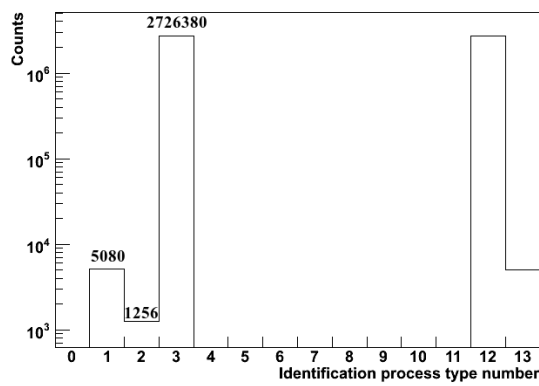


Figure 4.2: Identification process type for a polished surface.

In figure 4.1 we show a schematic representation of the polished surface and the possible processes.

Figure 4.2 shows the possible processes for this kind of finish. The list of the possible processes comprehends: undefined (0), refraction (1), fresnel reflection (2), total internal reflection (3), lambertian reflection (4), lobe reflection (5), spike reflection (6), backscattering (7), absorption (8), detection (9), not at boundary (10), same material (11), step too small (12), no rindex (13). The bin number shown between brackets represents each process (meaning of the numbers in the X-axis of the figure 4.2 ). In figure 4.2 we show that the 50% of the photons are refracted and the rest are absorbed by the material. Each time a fresnel reflection occurs several thousand of total internal reflections happens. For the total internal reflection process the photons stay inside the crystal bouncing, while for the fresnel reflection, after one photon is reflected is more probable that this photon be refracted in the next bounce. When the angles are below the critical angle part of the optical photons scape from the crystal and the other are reflected. But if the angles are bigger than the critical angle the photons bounce a few times in the crystal before being absorbed by the material. For this reason the number of total internal reflections is large compared with the number of

fresnel reflections.

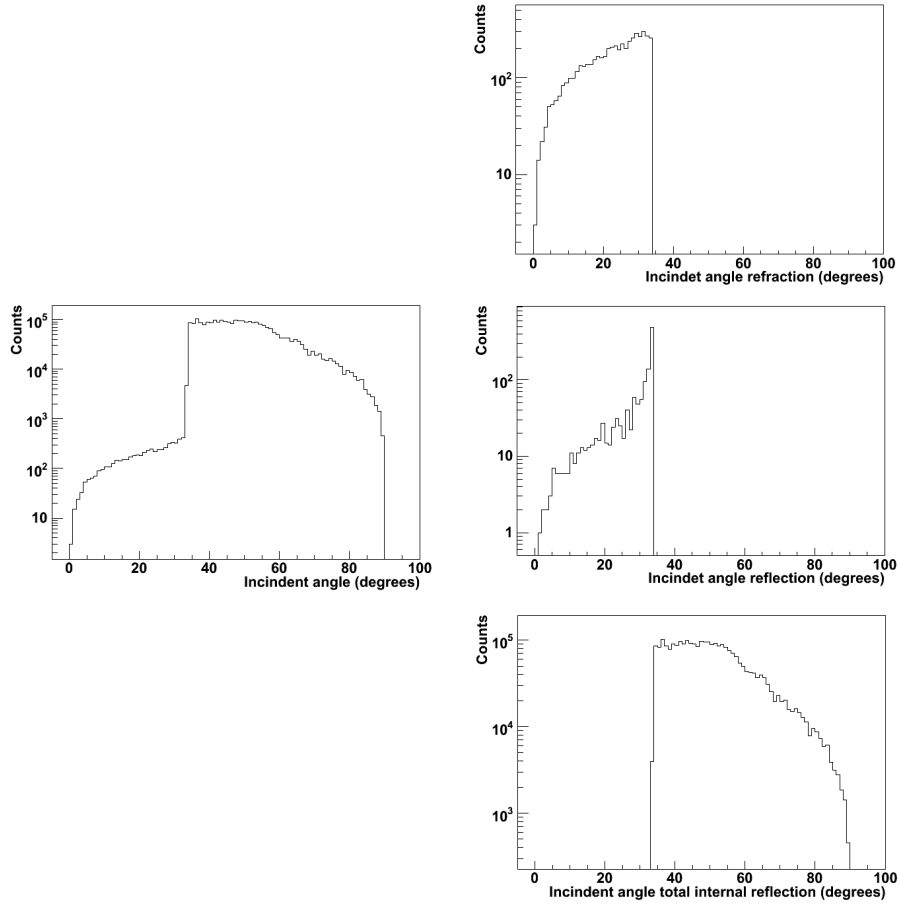


Figure 4.3: (a) Incident angle for a polished surface. (b) Incident angles for each process type in a polished surface.

In figure 4.3 (part a) we show the probability of incidence on a surface for a given angle and for all the processes. The angles values swept from  $0^\circ$  to  $90^\circ$ . To understand the distribution of the angles we need to understand what happens for each process. In the right part of figure 4.3 (part b) we show the same graph but for each individual process separately. In the first one we show the incident angles when the process happening is refraction. The angles take values between  $0^\circ$  and  $34^\circ$ . In chapter two we introduced some basics concepts on optics. If we focus in the concept of critical angle and we calculate this value for a photon going from a medium with refraction index of  $n_i = 1.79$  (CsI) to another with  $n_t = 1$  (air), we obtain a critical angle of  $34^\circ$  (see equation 4.1).

#### 4.1 Study of the light propagation in the crystal with Geant4. 17

$$n_i \sin \theta_c = n_t \sin 90^\circ \Rightarrow \theta_c = 34^\circ \quad (4.1)$$

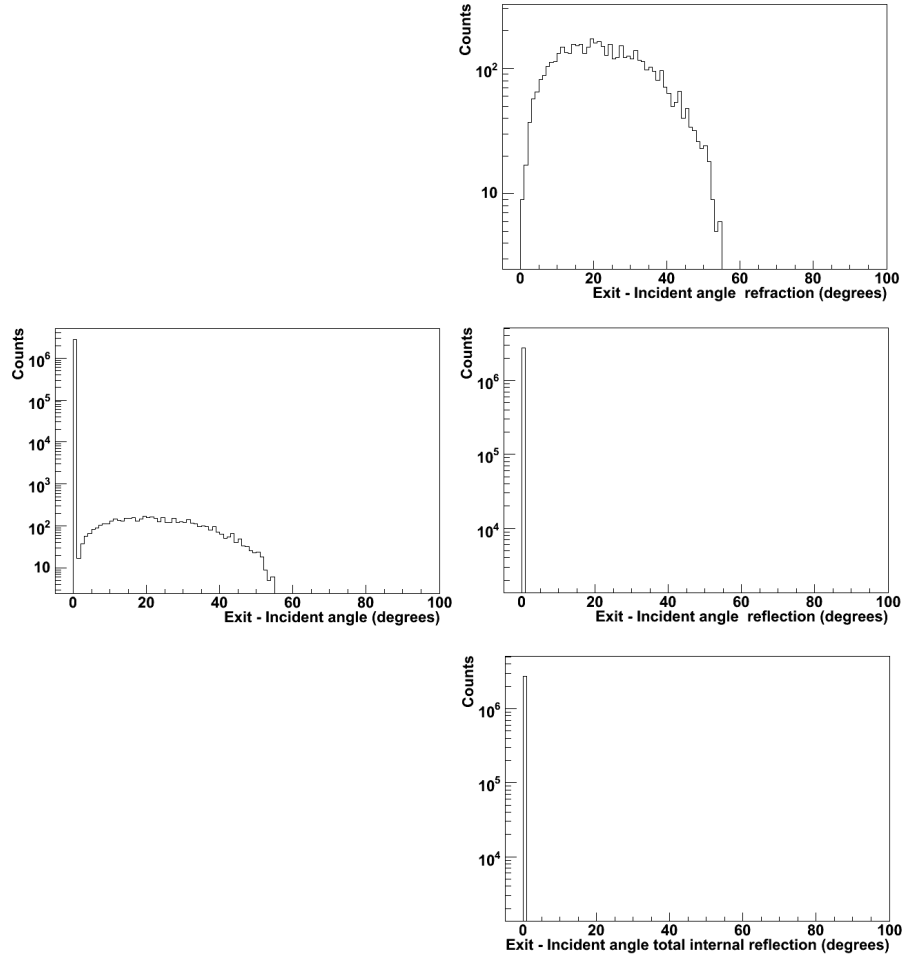


Figure 4.4: (a) Difference between the exit and incident angles for a polished surface. (b) Difference between the exit and incident angles for each process type in a polished surface.

So, above  $\theta_c = 34^\circ$  all the photons undergo total internal reflection, but for lower values the photons can be refracted or reflected. So the incident angles of the photons refracted goes from  $0^\circ$  to  $34^\circ$ . In the middle graph we have the incident angles for the photons reflected and as we had seen in the definition of the critical angle, these possible angles are below the critical. In the third one is showed the total internal reflection angles, and as we expected the angles go from  $34^\circ$  to  $90^\circ$ . In figure 4.3 (part a) we have a

big jump in the critical angle. This is because when total internal reflection happens the photon stay inside the crystal bouncing and each time we have a bounce the incident angle is above the critical, and for this reason we have less counts below the critical.

Figure 4.4 (a) shows the difference between the exit angle and the incident angle for all the processes. In the right side of figure 4.4 it is shown the difference for each individual process. For the refraction case (top on the right) we have a distribution between  $0^\circ$  and  $56^\circ$ . This value corresponds to the different between the incident and the exit angles distribution. The incident angles for the refraction process took values between  $0^\circ$  and  $34^\circ$ , the exit angles take values between  $0^\circ$  and  $90^\circ$ , this can be calculated using the refraction law. In the other two graphs we see the difference between the fresnel reflection and the total internal reflection. It is zero because the outgoing angle is the same than the incident angle.

### Polishedbackpainted:

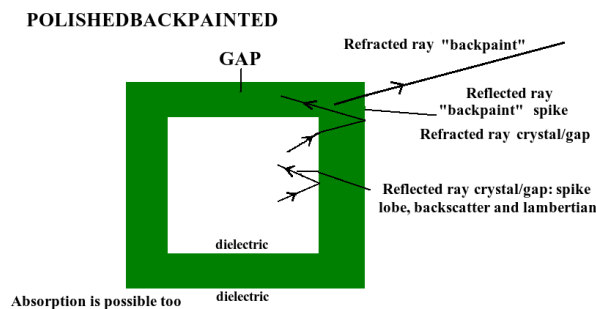


Figure 4.5: Schematic paint of a polishedbackpainted surface.

The polishedbackpainted surface tries to represent a polished surface with a specular reflector wrapping. In a polished "back paint" surface (between two dielectric media) the possible processes are: lobe reflection, spike reflection, lambertian reflection, backscatter reflection, absorption and refraction. "Back painted" stands for the description in simulation of the physical case corresponding to a wrapping around the scintillator surface, with an intermediate thin layer (as opposed to "frontpainted" where there is no such layer) between them. The "polished" finish trumps any other specification, we have a polished surface between the crystal and the gap and a polished backpaint, other parameters related with the roughness are ignored.

In figure 4.5 we show a schematic representation of the surface and some of the possible processes.

#### 4.1 Study of the light propagation in the crystal with Geant4. 19

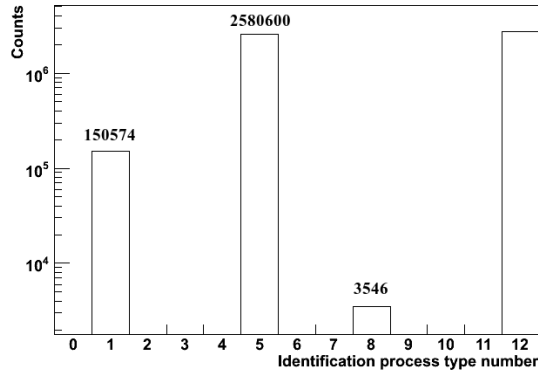


Figure 4.6: Identification process type for a polishedbackpainted surface.

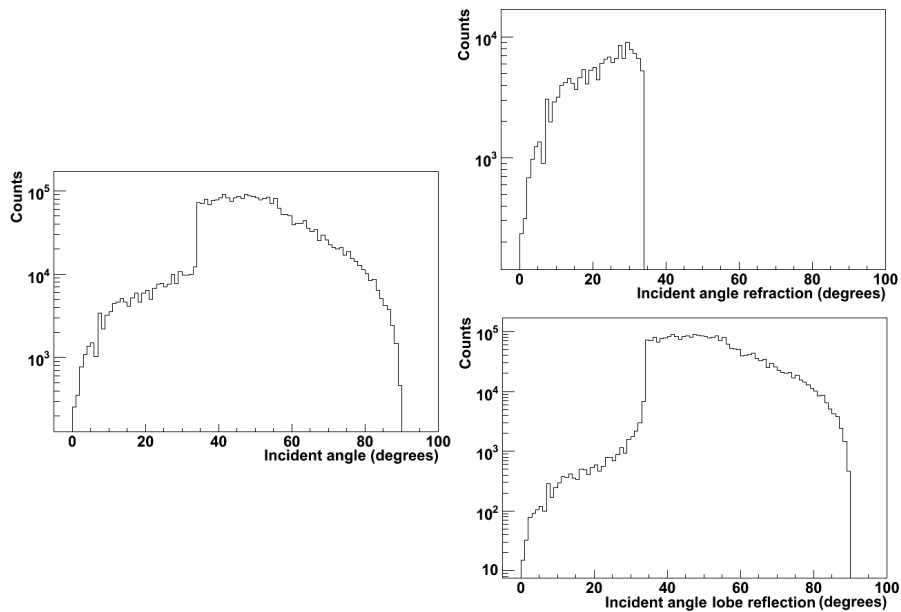


Figure 4.7: (a) Incident angle for a polishedbackpainted surface. (b) Incident angles for each process type in a polishedbackpainted surface.

Figure 4.6 shows the possible processes for this kind of finish. The 43.15% of the photons are absorbed by the boundary, after a mean number of lobe reflections per photon of the order of 33. With polishedbackpainted we have a polished surface between the crystal and the gap and a polished backpaint, so the photons can undergo lobe reflection in the surface between the crystal and the gap or in the backpaint. The optical photons are refracted in the

gap first, and can scape from the backpaint by refraction, too. So, we have more refractions than photons coming from the source and the number of lobe reflections is so high.

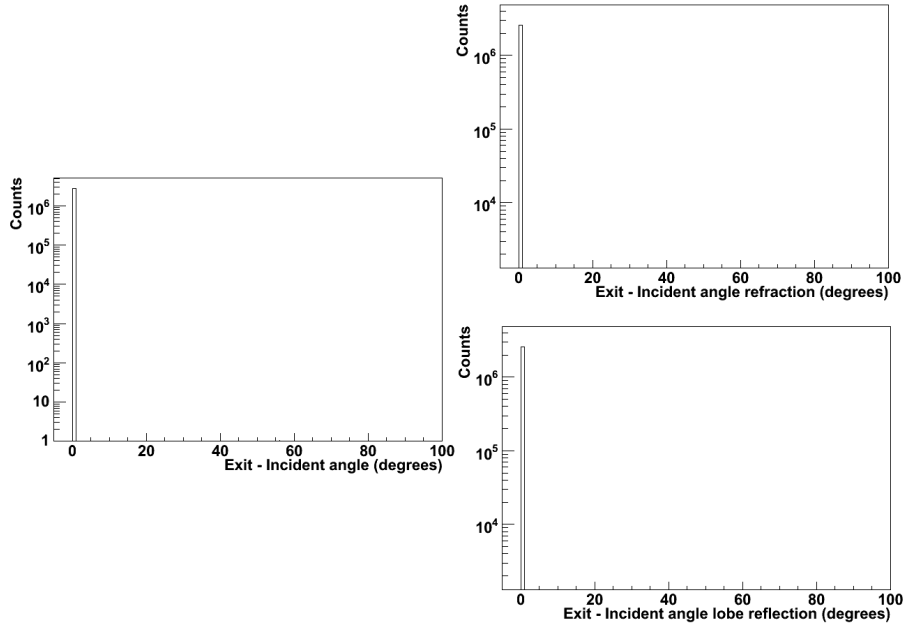


Figure 4.8: Difference between the exit and incident angles for the lobe reflection in a polished backpainted surface.

Figure 4.7 shows in the pad (a) the incident angles for all the processes happening in the boundaries of the box. The range of the incident angle is  $0^\circ$  to  $90^\circ$ . Part (b) shows the incident angles for the individual processes of refraction and lobe reflection. The refraction is only possible for incident angles below  $34^\circ$  because only below this value is possible that the photons scape from the crystal. The lobe reflection is possible for all the angles between  $0^\circ$  and  $90^\circ$ .

In the figure 4.8 we show the difference between the exit and incident angles for the lobe reflection process. As we expected this difference is zero because the incoming and outgoing angles are the same, the lobe reflection is specular.

### Polished frontpainted:

The polished frontpainted surface tries to represent a polished crystal with a diffuse reflector wrapping. In a polished top-layer paint surface (between

## 4.1 Study of the light propagation in the crystal with Geant4. 21

two dielectric media) the possible processes are: spike reflection and absorption. The “polished” finish trumps any other specification, the program ignores some other parameters.

In figure 4.9 we show a schematic representation of the surface and the possible processes.

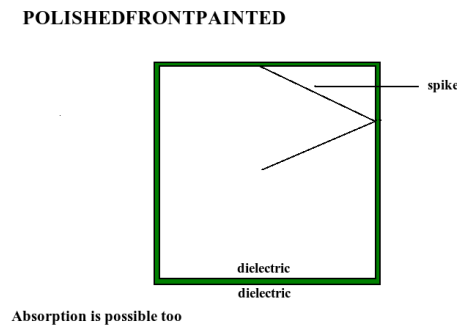


Figure 4.9: Schematic paint of a polishedfrontpainted surface.

Figure 4.10 shows the possible processes for this kind of finish. The 92% of the total photons are absorbed by the boundary. They are bouncing in the walls of the crystal having spike reflections until being absorbed, the most by the boundary, the other by the material.

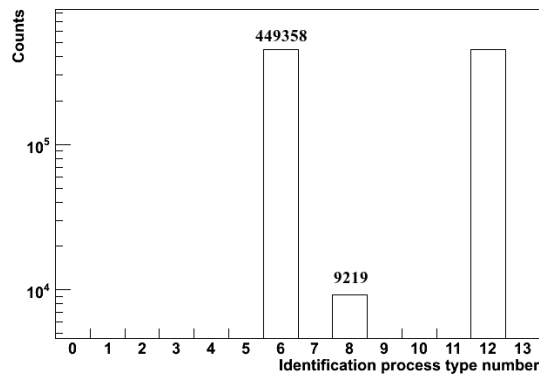


Figure 4.10: Identification process type for a polishedfrontpainted surface.

The incident angles of the photons goes from  $0^\circ$  to  $90^\circ$ . The distribution is continuous because the only reflection process happening is the spike reflection, for this kind of reflection all the angles are allowed, and the simulated source emit photons goes in random direction.

The difference between the exit and incident angles, as we expected is zero because the angles of incidence and exit are the same. Remember that the spike reflection is perfectly specular over the average surface.

### Ground:

The ground surface tries to represent an unpolished surface without wrapping. In a rough surface (between two dielectric media) the possible processes are: lobe reflection, spike reflection, lambertian reflection, backscatter and refraction. In figure 4.9 we show a schematic representation of the surface.

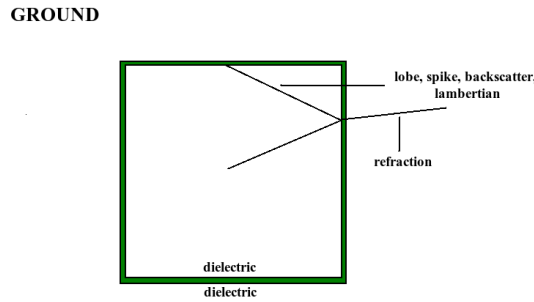


Figure 4.11: Schematic paint of a ground surface.

We use now rough surfaces and we have to take into account the sigma-alpha parameter. We are going to divide the next results in two cases, results with sigma-alpha zero and with sigma-alpha different from zero (we used a value ten). We divide these in another two options: specular lobe constant set to one and specular spike constant set to zero; or specular lobe constant set to zero and specular spike constant set to one. These combinations give us eight different cases (see table 4.1).

Processes	sl = 1 sa = 0	sl = 1 sa = 10	Processes	ss = 1 sa = 0	ss = 1 sa = 10
Refraction	5073	10479	Refraction	5143	10049
Lobe reflection	4249490	17205	Spike reflection	4218484	54661

Table 4.1: Probability for the possible processes in a ground surface in the next conditions: specular lobe (sl) set to one (specular spike (ss) set to zero) and sigma-alpha (sa) zero or ten. Specular spike set to one (specular lobe set to zero) and sigma-alpha zero or ten.

## 4.1 Study of the light propagation in the crystal with Geant4. 23

Table 4.1 shows the proportions of the different processes happening in the possible cases. Increasing the sigmaalpha parameter the number of refractions increases in both cases, specular lobe one or specular spike one. The lobe reflection decreases with the increment of the sigmaalpha, because more photons escape from the crystal. Now, rays that would have otherwise been bouncing around (continued reflection) can now escape the crystal (for being a ground surface).

### GroundBackPainted:

The groundbackpainted surface tries to represent a rough surface with a specular reflector wrapping. In figure 4.12 we show in a schematic representation of the surface.

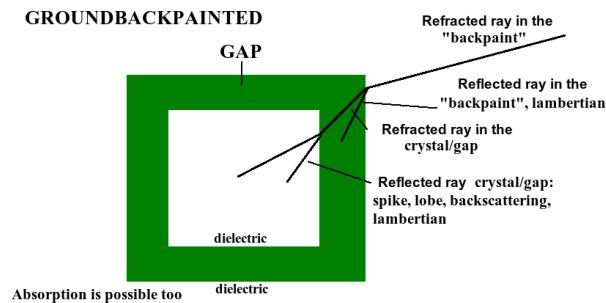


Figure 4.12: Schematic paint of a groundbackpainted surface.

Processes	sl = 1 sa = 0	sl = 1 sa = 10	Processes	ss = 1 sa = 0	ss = 1 sa = 10
Refraction	193124	385197	Refraction	185604	274158
Lobe reflection	4348400	684008	Spike reflection	4547331	16112056
Absorption	4422	8013	Absorption	4296	7179

Table 4.2: Probability for the processes happening in a groundbackpainted surface in the next conditions: specular lobe set (sl) to one (specular spike(ss) set to zero) and sigmaalpha (sa) zero or ten. Specular spike set to one (specular lobe set to zero) and sigmaalpha zero or ten.

Table 4.2 shows the frequency of all the processes happening in this surface. We show that when we increased the sigmaalpha, independently of the specular constants values the number of refractions is bigger, consequently the number of reflections decreased because more photons escape from the crystal. The number of absorptions is being increased due to the roughness.

### GroundFrontPainted:

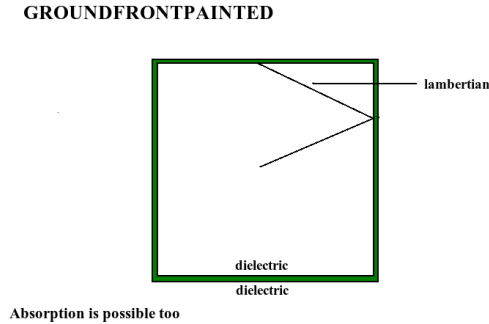


Figure 4.13: Schematic paint of a groundfrontpainted surface.

The groundfrontpainted surface tries to represent an unpolished surface with a diffuse reflector. In a rough top-layer paint surface (between two dielectric media) the possible processes are: lambertian reflection and absorption. Whatever you set for sigmaalpha make no difference, the reflection is always lambertian.

In figure 4.13 we show in a schematic representation of the surface.

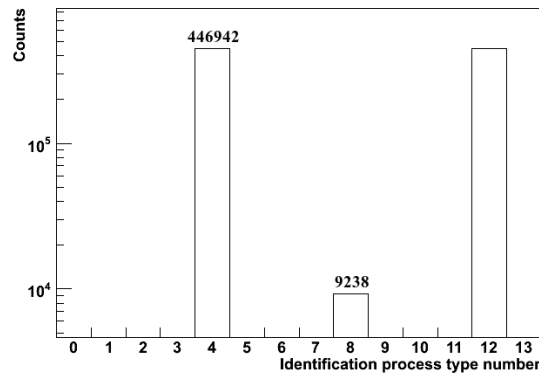


Figure 4.14: Identification process type for a groundfrontpainted surface.

Figure 4.14 shows the possible processes for this kind of finish. The photons are bouncing in the walls until being absorbed by the boundary most of them, a percent of 92%. In this figure we only show processes related with the boundary, i.e. some photons absorbed by the material are not represented in this graph.

The incident angles goes from  $0^\circ$  to  $90^\circ$ , the only type of reflection happening for this surface is the lambertian, and this can occur for each angle between  $0^\circ$  and  $90^\circ$ . So, we observe a continuous distribution.

In figure 4.15 is showed the difference between the incident and exit angles for the photons. This difference is non zero because the exact form of the reflection depends on the structure of the surface. The reflected light is scattered in all directions.

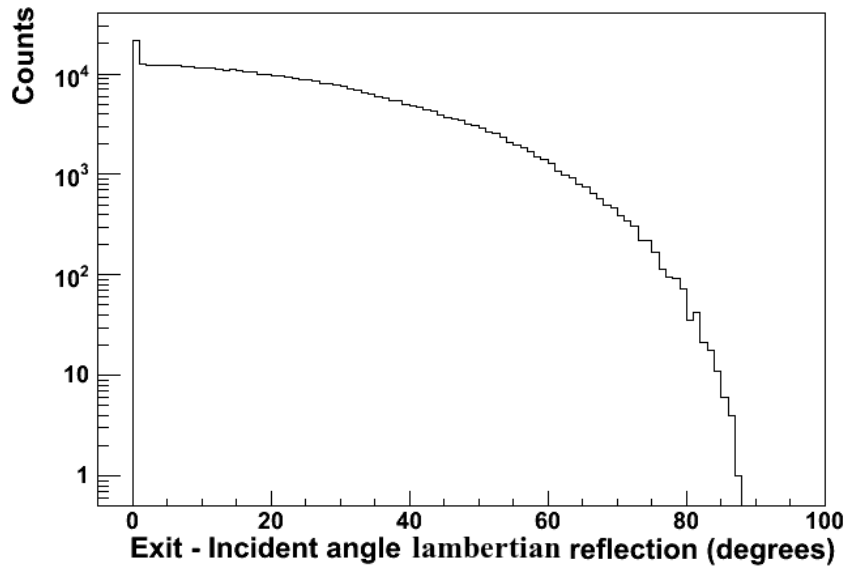


Figure 4.15: Difference between incident and exit angles for a groundfront-painted surface.

## 4.2 Simulation of the crystal prototypes.

The calorimeter for in flight detection of  $\gamma$ -rays and light charged particles is one of the main detection systems of the R3B experiment [10] at FAIR. This detector will be used in most of the physical cases presented in the R3B Technical proposal [10], though the requirements differ significantly from one case to the other. The selection of the appropriate scintillation material, the crystals shape and the readout device are critical parameter that would determined the nominal energy resolution of the detector. CsI(Tl) crystals coupled to adequate sensors (APD or PM) resolution (lower than 5% for 662 keV  $\gamma$ 's) could be a plausible solution, at least for backward angles.

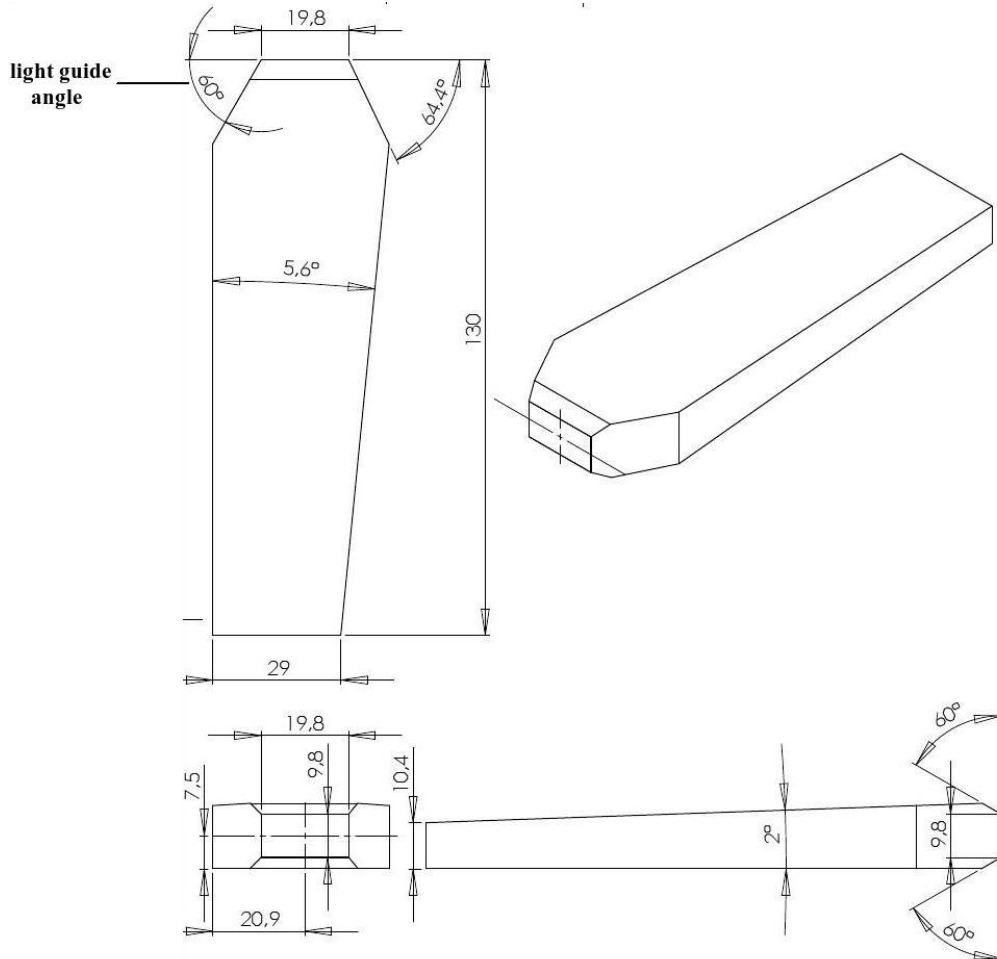


Figure 4.16: Geometry of the prototype designed by the GENP.

Due to a certain features that the calorimeter has to have, some of the characteristics of the crystals are fixed, like the length and the areas of the superior and inferior parts. According to this a prototype for the crystals of the calorimeter CALIFA (see figure 4.16) has been designed . The idea of this shape is guide the light to the superior part and cover all the solid angle with the adequate segmentation, for this reason the crystals are formed by two trapezoids. The function of the superior trapezoid is guide the light towards the detection system. In this section, we study how a change in the light guide angle (see figure 4.16) affects to the light collected in the detectors. We only simulate two finishes types, because these two have the most opposite features and could be a good candidates for the real crystals.

One is a diffuse reflector and the other is a specular reflector.

In our simulation we implement the crystal in Geant4 by combination of two trapezoids. Simple solids can be combined using Boolean operations. For example, two trapezoids can be combined with the union Boolean operation. We made a simplification, we eliminate the longitudinal chamfers, because they are not going to be decisive in the light collection.

#### 4.2.1 Dependences with the light guide angle for a source of gammas.

In the next sections we are going to check how is the behaviour of the light collection, when the light guide angle is modified. We are going to use a gamma generator.

The simulations made in this section and in the next, had the next features:

- Beam of 1000 gammas with the next directions (see figure 4.17). Gammas parallel to the Z-axis (length of the crystals) and in a uniform way in all the entrance face.

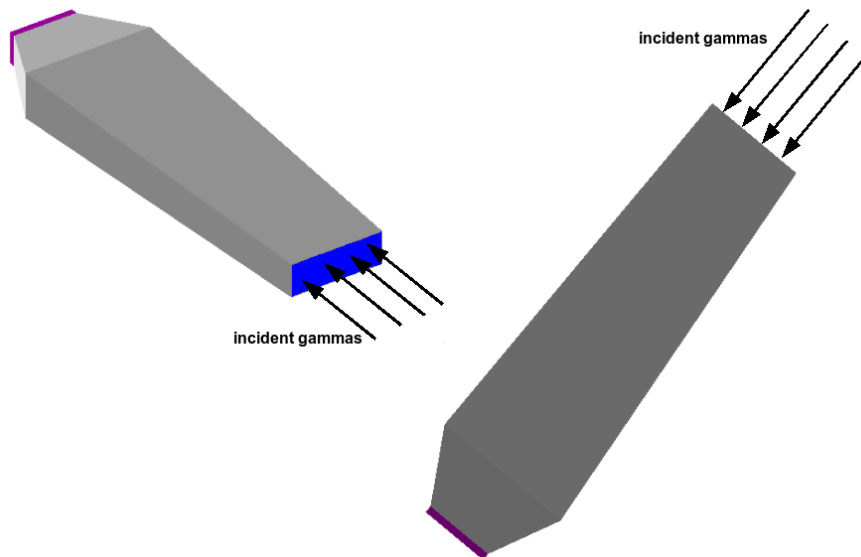


Figure 4.17: View of the gamma beam.

- Energy of the gammas 0.662 keV
- Finish: polishedbackpainted and groundfrontpainted

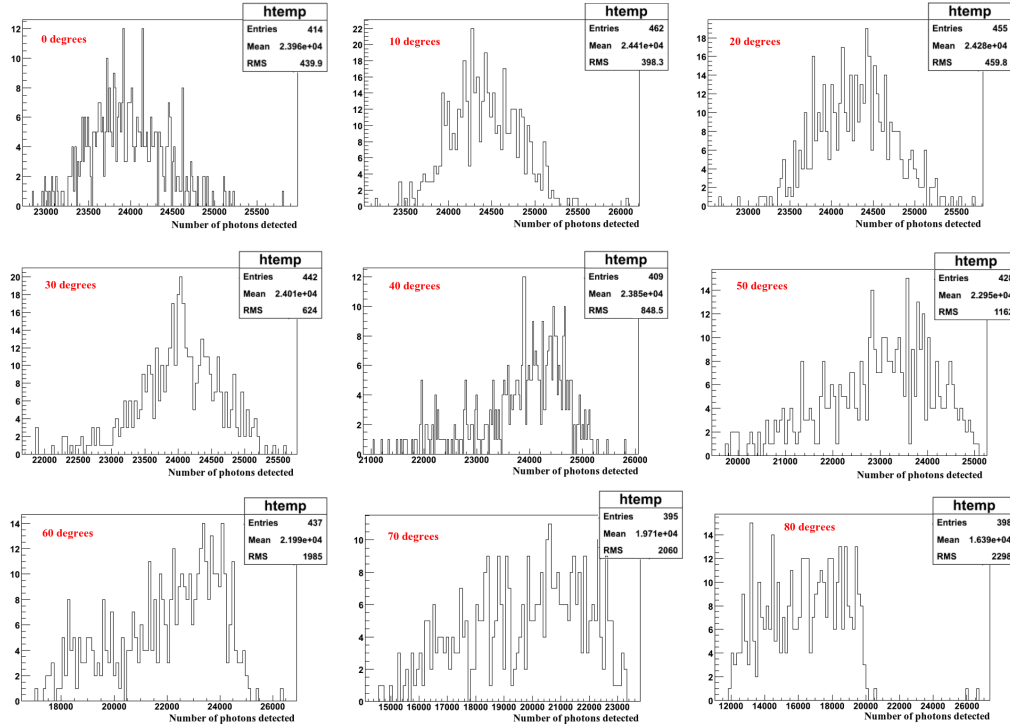


Figure 4.18: Number of detections for each light guide angle doing a cut in 0.660 keV. Surface finish polishedbackpainted.

### Polishedbackpainted finish

In figure 4.18 we show the number of detections for some angles of the light guide when the energy deposited by the gamma is more than 0.660 MeV. Using this cut we discard photons that are not depositing their full energy in the crystal.

In next figure (see figure 4.19) we see the mean number of detections for each angle between  $0^\circ$  and  $80^\circ$ . What we see is that when you increase the angle of the light guide, the number of photons detected is constant until  $40^\circ$  and then begin to decrease. The error used in this figure is the RMS showed in the figure above, this is a statistical measure of the magnitude of a varying quantity, not exactly an error. To completely understand this behaviour we need to study another processes happening in the polishedbackpainted surface.

In figure 4.20 we show the number of lobe reflections when the energy deposited by the gamma is more than 0.660 MeV for angles going from  $0^\circ$  to  $80^\circ$ . The number of reflections is a very important parameter to understand why the number of photons detected is bigger for low values of the light

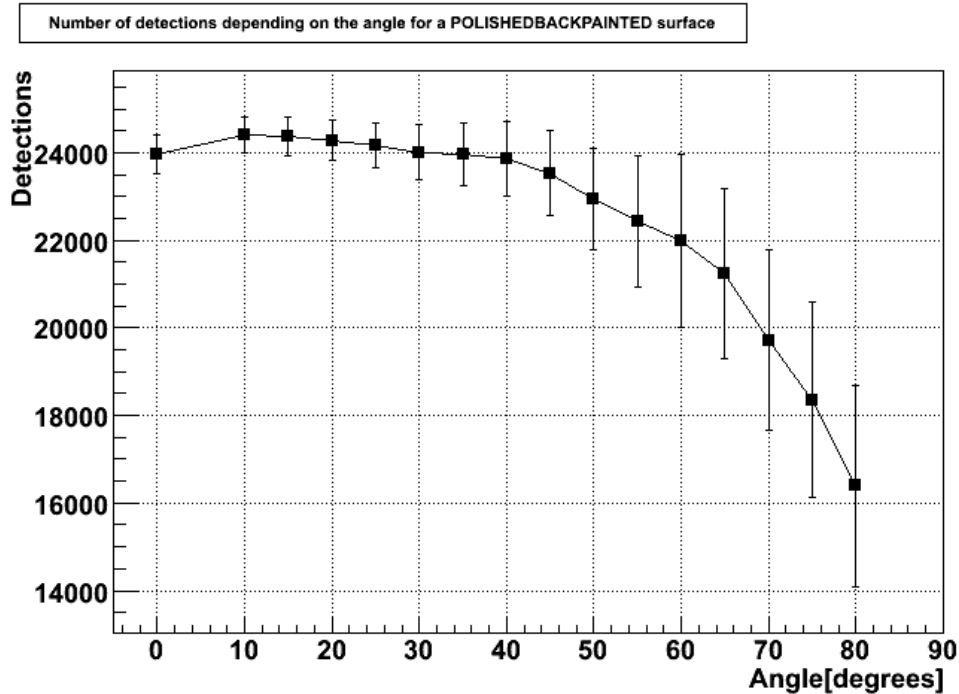


Figure 4.19: Number of detections depending on the light guide angle. Surface finish polishedbackpainted.

angle. The distributions of lobe reflections are well defined up to  $20^\circ$ , here the distributions begins to deform and they are more uniform, there is no a clear maximum. What is happening is that when we have a low value of the light guide angle, the upper part of the crystal (the light guide) is shorter than when the angles are bigger. So, this longer part do the photons go back into the crystal and more reflections happen. We will see the consequences of having more reflections using the next four figures and how this fact affect to the number of optical photons arriving to the detector.

In figure 4.21 we see the behaviour of the lobe reflections depending on the angle. The values in the y-axis are the mean number of lobe reflections with their corresponding error RMS, taken from the figure 4.20.

In figure 4.22 we see the distributions of the number of refractions happening when the energy deposited by the gamma is more than 0.660 MeV. The next figure (see 4.23) show to us how the number of refractions varies depending on the angle. We see that these values increasing when we increase the angle of the light guide. Remember that for larger values of the angles the probability of lobe reflection is bigger, so the photons rebound more times in the surfaces and the possibility of going out the surface becomes higher.

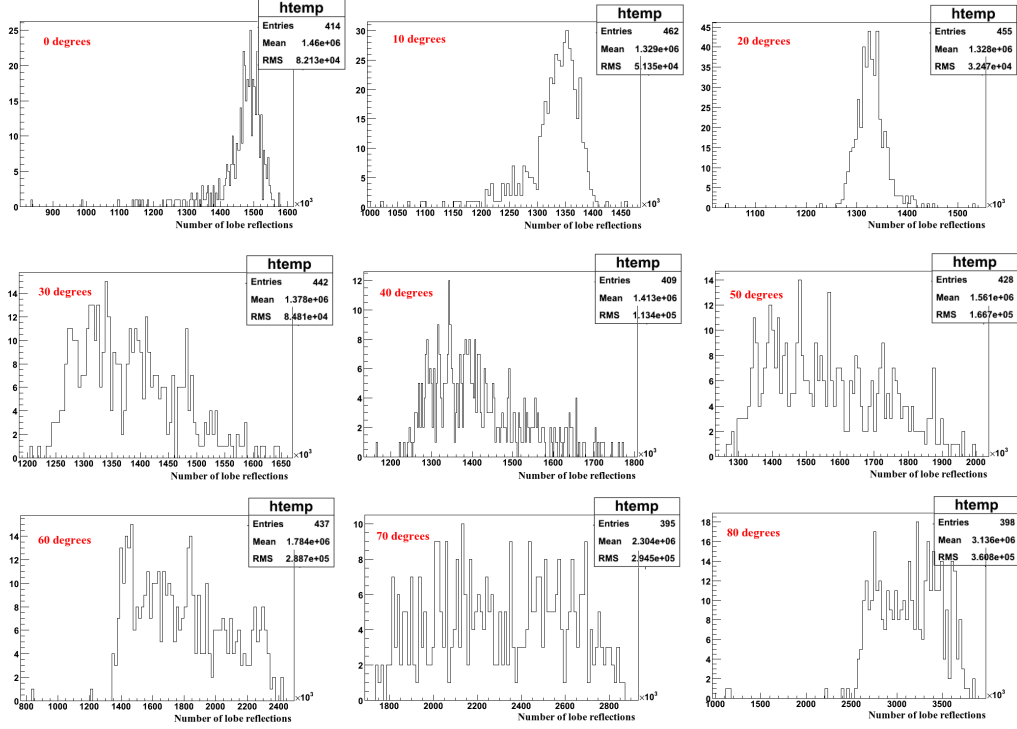


Figure 4.20: Number of lobe reflections for each light guide angle doing a cut in 0.660 keV. Surface finish polishedbackpainted.

### Groundfrontpainted finish

Now we are going to study the light guide angle effect for another kind of finish, the groundfrontpainted. This finish represents a diffuse reflector. We are going to study the number of photons detected, the number of lambertian reflections and the number of absorptions depending on the light guide angle. In figure 4.24 we see the number of detections for some particular angles when the energy is bigger than 0.660 MeV. Figure 4.25 shows the number of detections for each angle (energy deposited bigger than 0.660 MeV), we see that the number of photons detected is constant until  $55^\circ$ , after this value begins to decrease. This surface finish has the same behaviour that a polishedbackpainted surface.

In figure 4.26 we see the number of lambertian reflections for some particular angles when the energy is over 0.660 MeV. In figure 4.27 we show the number of lambertian reflections for each angle. After  $55^\circ$  the number of lambertian reflections is being incremented and the particles give more rounds inside the crystal, so as a consequence of this, the number of detections is smaller because when the number of hits in the crystal walls increase, the

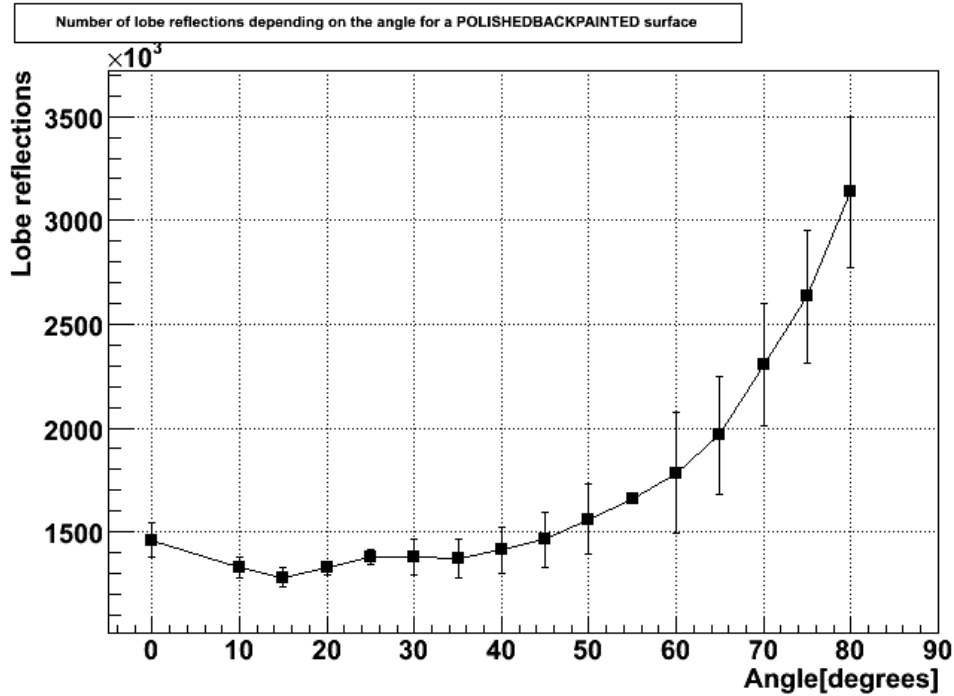


Figure 4.21: Number of lobe reflections depending on the light guide angle. Surface finish polishedbackpainted.

probability of one photon be absorbed in the boundary or in the material is bigger.

4.28 and 4.29) when we are over  $55^\circ$ . Same cut was used in these two plots.

Another fact that do the number of detections becoming smaller is the increasing in the number of absorptions (see figures

All these things do that the best angle for a higher light collection be one below  $55^\circ$ .

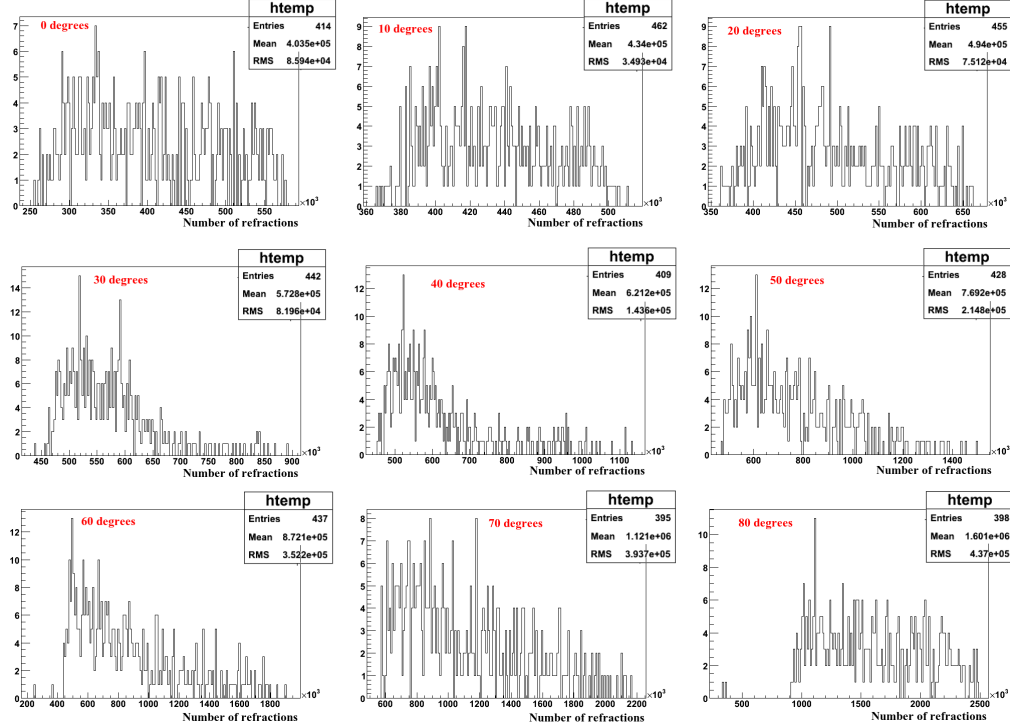


Figure 4.22: Number of refractions for each light guide angle doing a cut in 0.660 keV. Surface finish polishedbackpainted.

## 4.2.2 Dependences with the light guide angle for a source of photons.

All the results obtained in the previous subsections were checked too for a different simulated source, in these case the source used, emitted photons. The features of these simulations were the next.

- Simulated source emitting  $10^5$  optical photons with random directions and random positions. The distribution of the position is inside a cube of  $1\text{mm}^3$  situated 5 mm far from the crystal entrance face and with coordinates  $x, y$  being zero.
- Energy of the photons 3 eV

### Polishedbackpainted finish

Figure 4.30 shows the number of detections depending on the angle, for the simulation conditions seen before and for a surface finish polishedbackpainted. We observe the same behaviour than in the cases of a gamma source. For higher values of the angle, the number of detections decrease.

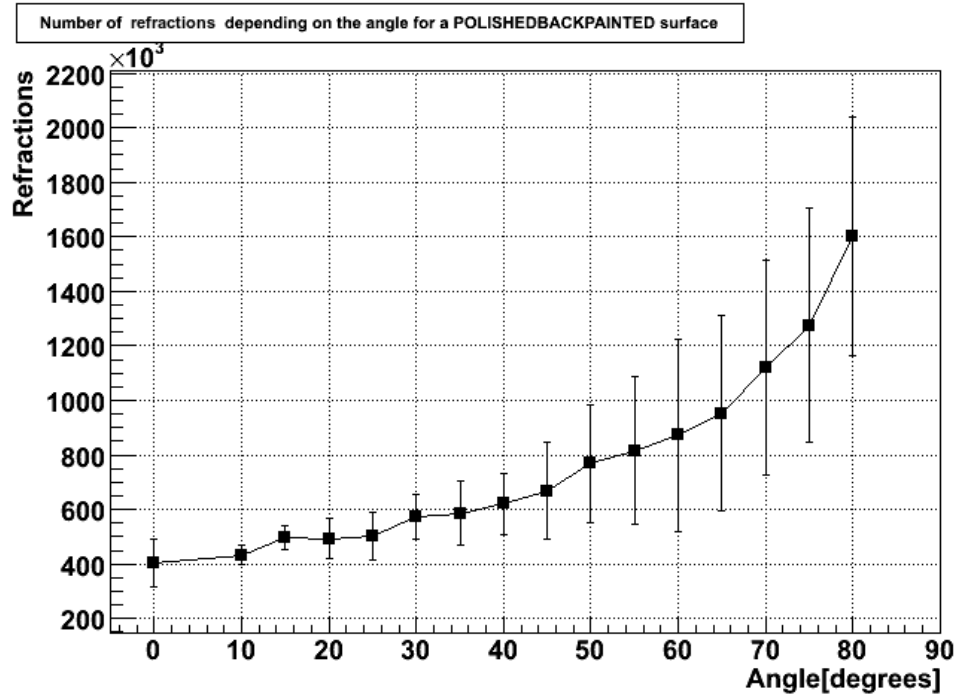


Figure 4.23: Number of refractions depending on the light guide angle. Surface finish polishedbackpainted.

The figure 4.31 shows how is the photon's behaviour for two different angles, and we see the "funnel effect". When the light guide angle is 80 degrees, right part of the figure, we see that the photons bounce more times the walls and it is more difficult for them arrive to the detector.

#### Groundfrontpainted finish

In the figure 4.32 we show the number of detections depending on the angle, for the simulation conditions seen before and for a groundfrontpainted finish. For higher values of the angle, the number of detections decrease.

Observing the figures 4.19 and 4.25 for the gamma source and the figures 4.30 and 4.32 . We can conclude that the dependence with the angle does not depend on surface finish or on the kind of source.

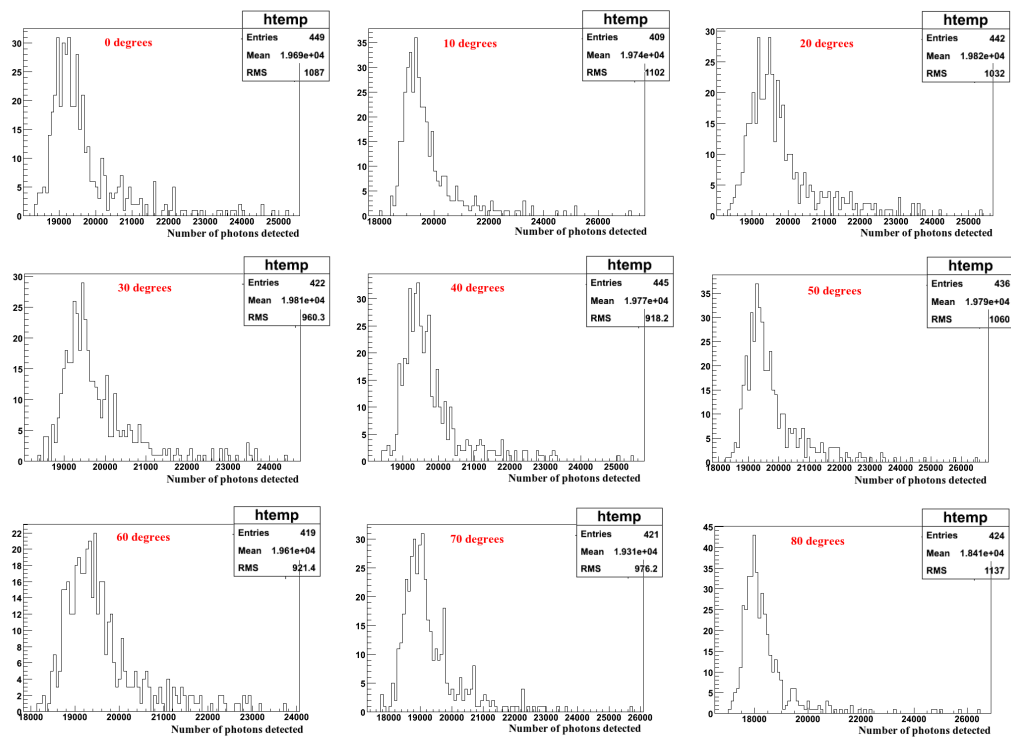


Figure 4.24: Number of detections for each light guide angle doing a cut in 0.660 keV. Surface finish groundfrontpainted.

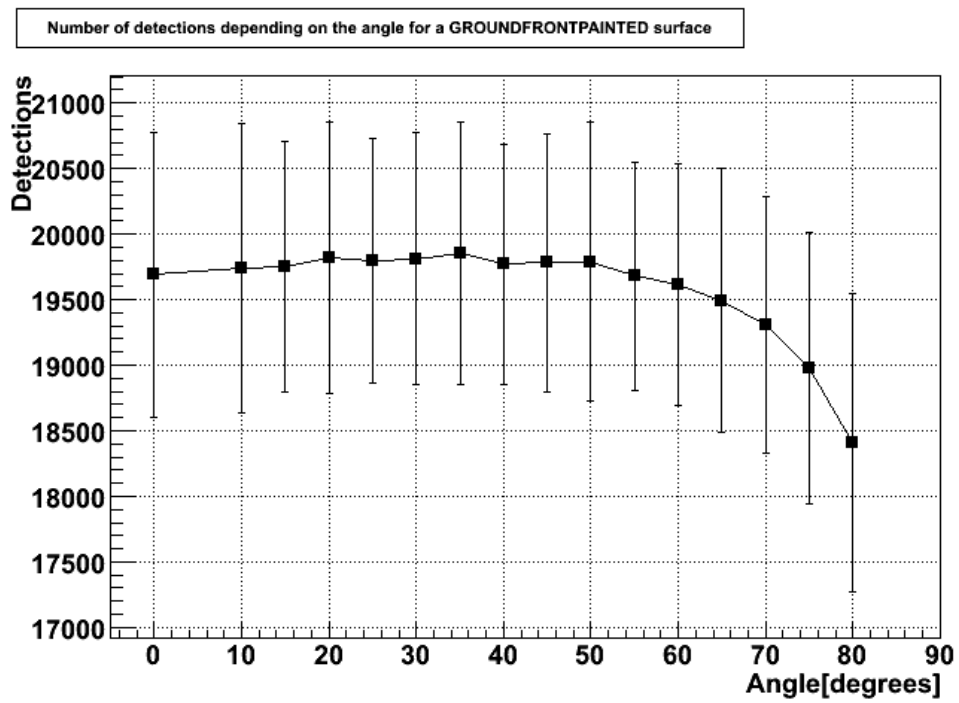


Figure 4.25: Number of detections for each light guide angle. Surface finish groundfrontpainted.

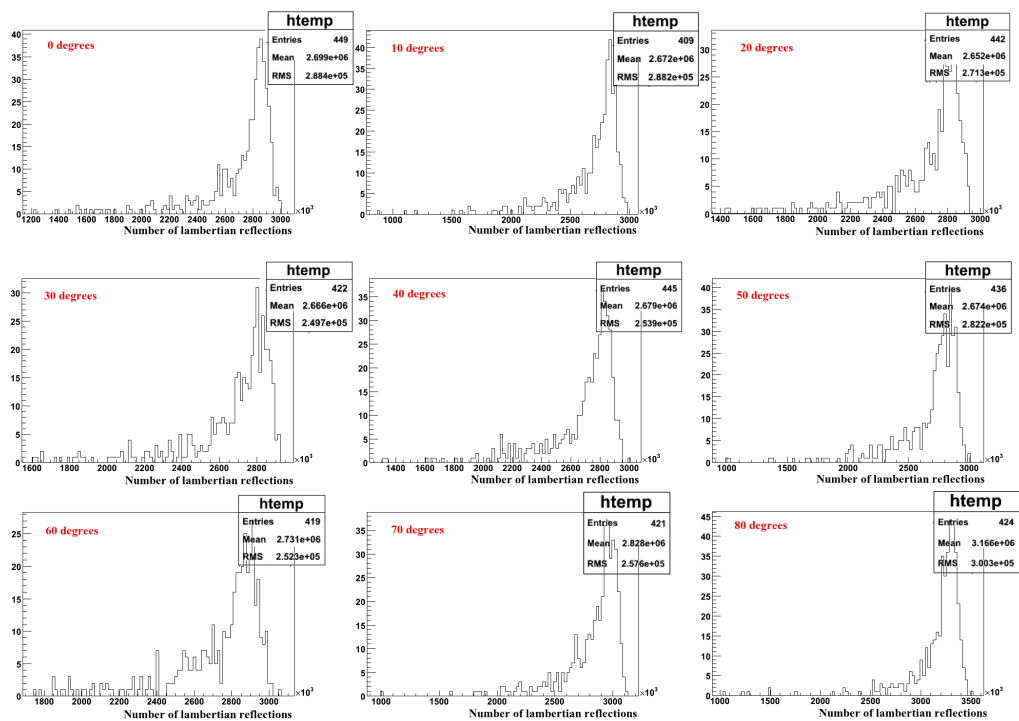


Figure 4.26: Number of lambertian reflections for each light guide angle doing a cut in 0.660 keV. Surface finish groundfrontpainted.

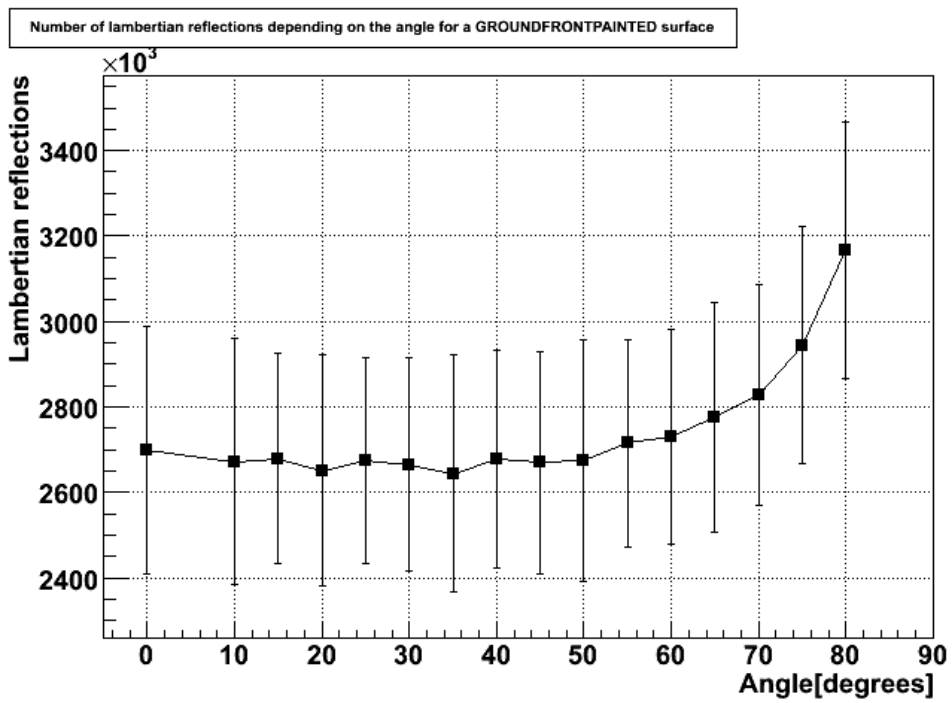


Figure 4.27: Number of lambertian reflections for each light guide angle. Surface finish groundfrontpainted.

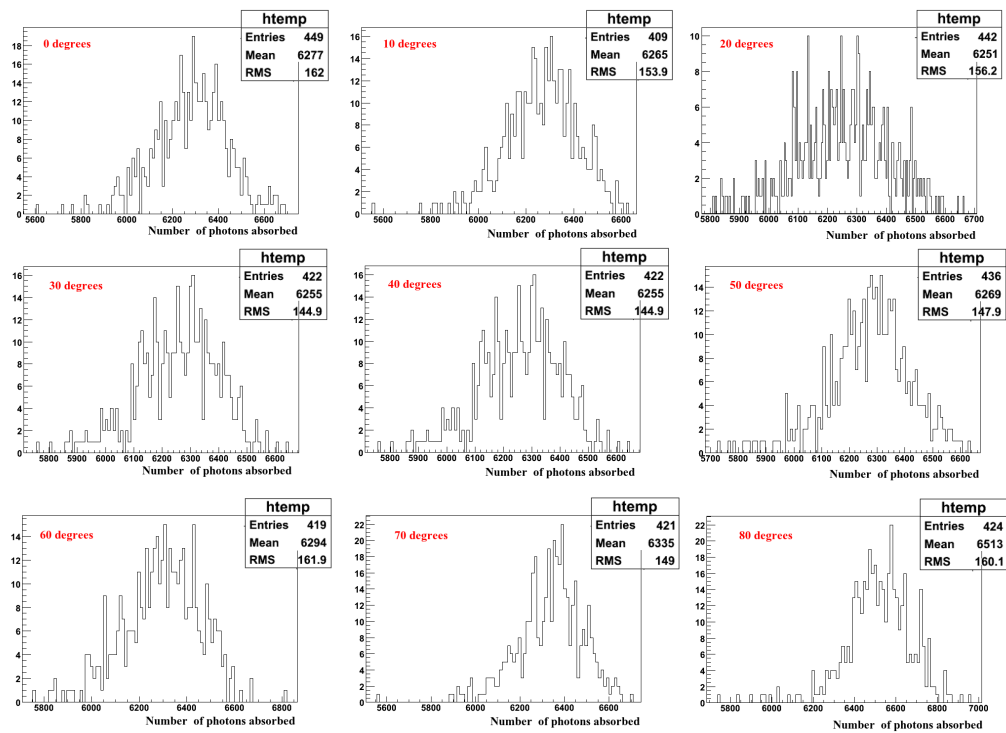


Figure 4.28: Number of absorptions for each light guide angle doing a cut in 0.660 keV. Surface finish groundfrontpainted.

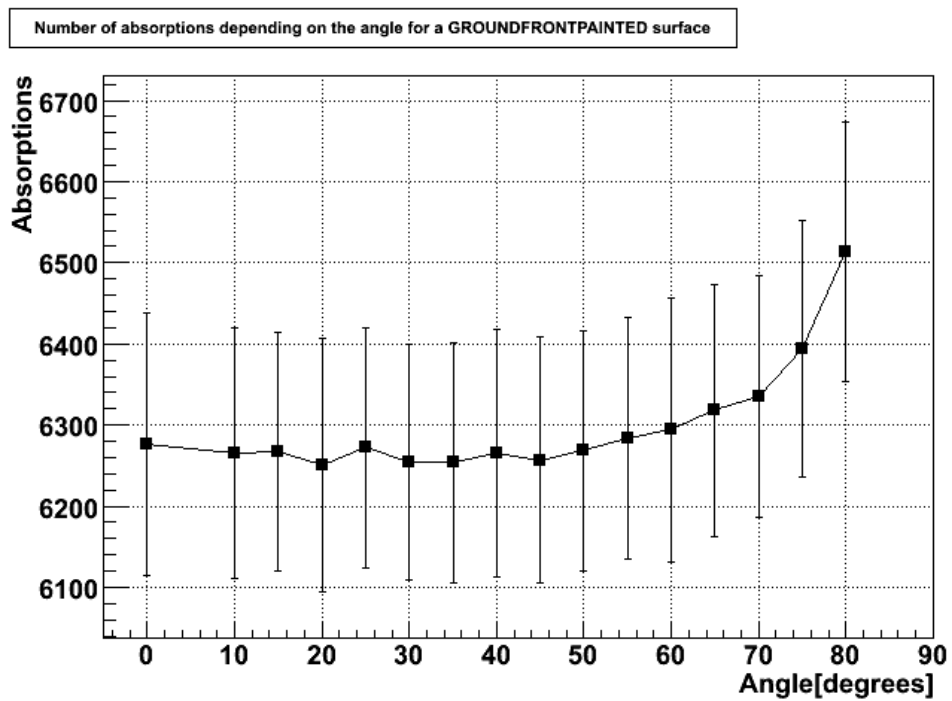


Figure 4.29: Number of absorptions for each light guide angle. Surface finish groundfrontpainted.

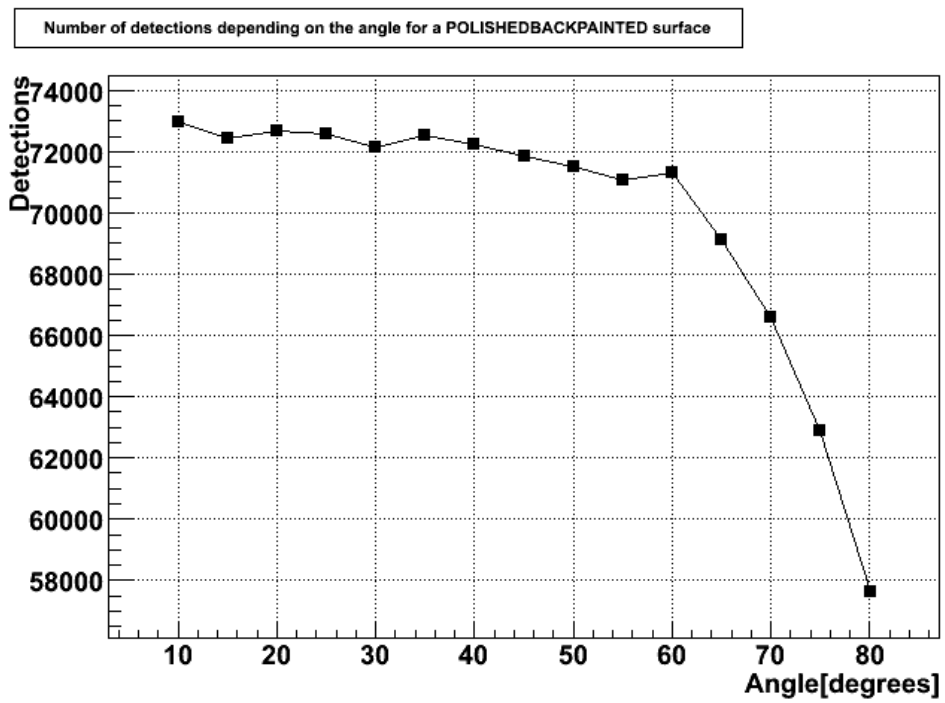
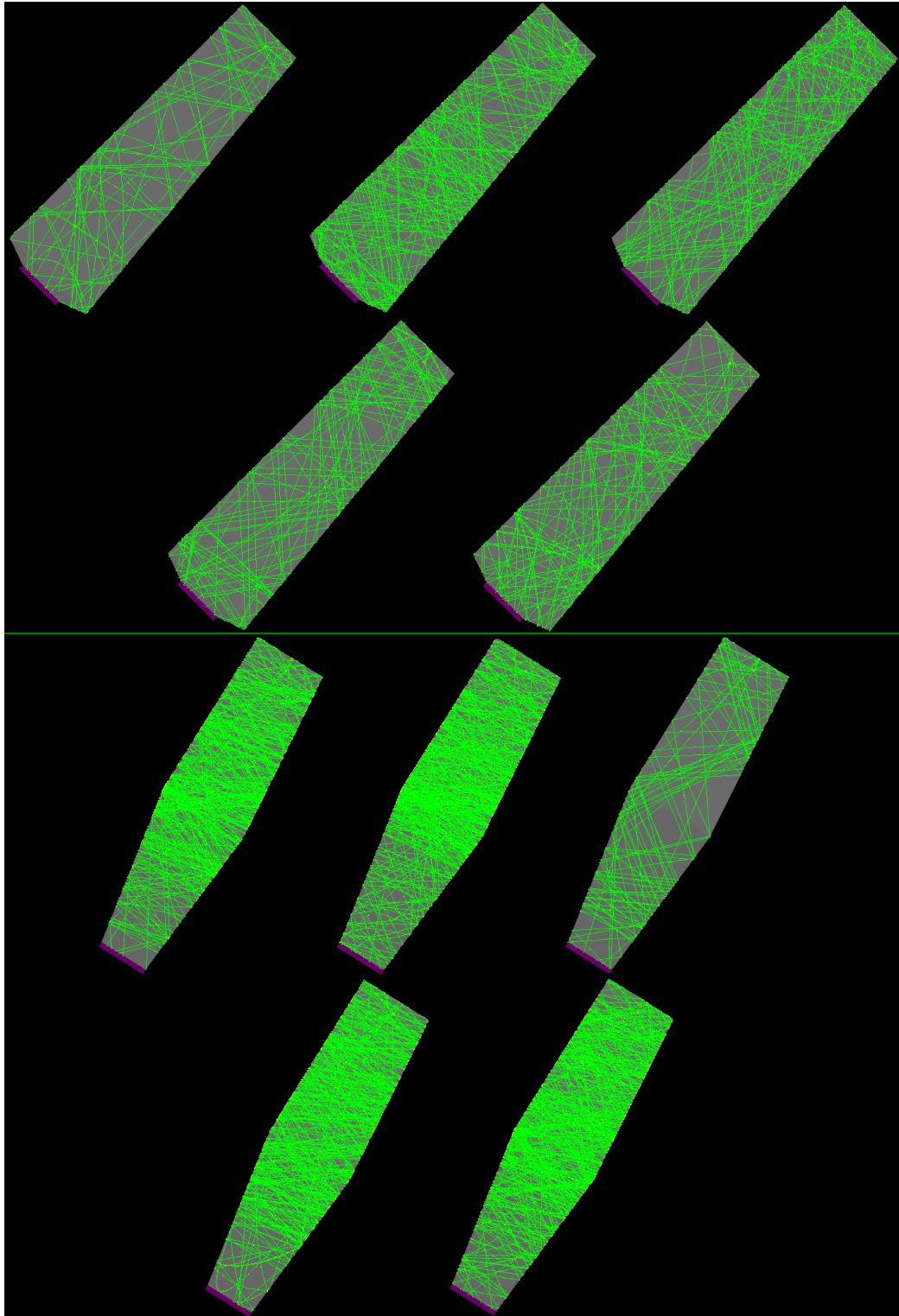


Figure 4.30: Number of detections for photons. Surface finish polishedback-painted.



*Figure 4.31:* In the top part of this picture we have the crystal with a light guide angle of 20 degrees and in the bottom with 80 degrees. In all the cases we show the propagation of ten photons inside the crystal.

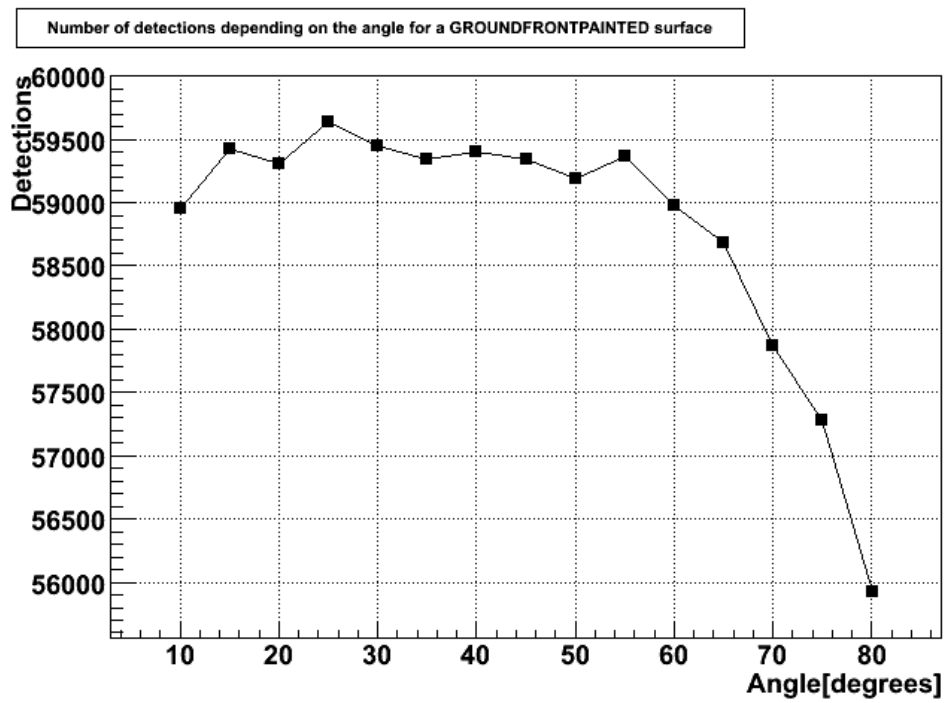


Figure 4.32: Number of detections for photons. Surface finish groundfront-painted.

# Chapter 5

## Conclusions

In this work we have described a general purpose simulation package based in Geant4 called R3BSim that can be used for the future R3B setup at FAIR, and also for the previous design.

The simulation provides the whole description of the different detectors (material, location and response) as well as the physical processes that take place during the experiment. All the processes events are recorded in root files that can be analysed externally.

We have applied the simulation to the study of the light propagation and collection in the crystals prototype of the calorimeter CALIFA. We can summary some conclusions:

- We understand the Geant4 treatment of the optics and how the program models real cases of scintillators and wrappings. We have tested all the Geant4 possibilities for the surface finish to understand the light propagation inside a CsI scintillator.
- We have also studied the reflectivity making a comparison with experimental data in order to fix it.
- We used the most different surface finish (ground-front-painted and polished-back-painted) to know how changes in the light guide geometry of the crystals varies the number of photons detected. To study this changes we used two different generators, given both the same results. In one case the beam was formed by gammas and in the other by photons. The results obtained was the same for the two finish. We can conclude that for high values of the light guide angle less photons are detected, because they go back into the crystal.

We conclude that the simulation is a powerful tool that can be used in the design of crystals for detector.



# Bibliography

- [1] Eugene Hecht, “Optics”, Addison Wesley, 2002, San Francisco
- [2] FAIR, [http://www.gsi.de/fair/index\\_e.html](http://www.gsi.de/fair/index_e.html)
- [3] Glenn F. Knoll, “Radiation Detection and Measurement”, John Wiley & sons, 2000, Ann Arbor
- [4] A. Levin and C. Moisan, “A more physical approach to model the surface treatment of scintillation counters and its implementation into DETECT”, TRIUMF Preprint TRI-PP-96-64, Oct. 1996
- [5] Martin Janecek and William W. Mosses, “Simulating scintillator light collection using measured optical reflectance”, TNS-00249-2009.R1, IEEE Transactions on Nuclear Science
- [6] Geant4 Collaboration, “Geant4 User’s Guide for Application Developers”, <http://geant4.web.cern.ch/geant4/support/index.shtml>
- [7] C. R. Nave, HyperPhysics, Department of Physics and Astronomy, Georgia State University, Atlanta (<http://hyperphysics.phy-astr.gsu.edu/>)
- [8] Geant4 Collaboration, “Physics reference Manual”, <http://geant4.web.cern.ch/geant4/support/index.shtml>
- [9] Geant4 User Forum “Processes Involving Optical Photons”, <http://hypernews.slac.stanford.edu/HyperNews/geant4/cindex>
- [10] Collaboration of R<sup>3</sup>B, “Technical Proposal for the Design, Construction, Commissioning and Operation of R<sup>3</sup>B”, [http://www.gsi.de/forschung/kp/kr/R3B/Documents\\_e.html](http://www.gsi.de/forschung/kp/kr/R3B/Documents_e.html).
- [11] W.R. Leo, “Techniques for Nuclear and Particle Physics Experiments”, Springer-Verlag, 1987, Laussane (Switzerland)

- [12] Collaboration of R<sup>3</sup>B, “Technical status report for CALIFA”, 2008, [www.iem.cfmac.csic.es/departamentos/nuclear/fnexp/r3b/CALIFA-TSR.pdf](http://www.iem.cfmac.csic.es/departamentos/nuclear/fnexp/r3b/CALIFA-TSR.pdf)
- [13] Saint Gobain data sheet, “CsI(Tl), CsI(Na) Cesium Iodide Scintillation Material”